Huan Yu[1]
Department of Mechanical and Aerospace Engineering,
University of California, San Diego,
La Jolla, CA 92093
e-mail: huy015@ucsd.edu

Shumon Koga
Department of Electrical and Computer Engineering,
University of California, San Diego,
La Jolla, CA 92093
e-mail: skoga@ucsd.edu

Tiago Roux Oliveira
Department of Electronics and Telecommunication Engineering,
State University of Rio de Janeiro (UERJ),
Rio de Janeiro 20550-900, Brazil
e-mail: tiagoroux@uerj.br

Miroslav Krstic
Department of Mechanical and Aerospace Engineering,
University of California, San Diego,
La Jolla, CA 92093
e-mail: krstic@ucsd.edu

Extremum Seeking for Traffic Congestion Control With a Downstream Bottleneck

This paper develops boundary control for freeway traffic with a downstream bottleneck. Traffic on a freeway segment with capacity drop at outlet of the segment is a common phenomenon that leads to traffic bottleneck problem. The capacity drop can be caused by lane-drop, hills, tunnel, bridge, or curvature on the road. If incoming traffic flow remains unchanged, traffic congestion forms upstream of the bottleneck since the upstream traffic demand exceeds its capacity. Therefore, it is important to regulate the incoming traffic flow of the segment to avoid overloading the bottleneck area. Traffic densities on the freeway segment are described with the Lighthill–Whitham–Richards (LWR) macroscopic partial differential equation (PDE) model. The incoming flow at the inlet of the freeway segment is controlled so that the optimal density that maximizes the outgoing flow is reached and the traffic congestion upstream of the bottleneck is mitigated. The density and traffic flow relation at the bottleneck area, usually described with fundamental diagram, is considered to be unknown. We tackle this problem using extremum seeking (ES) control with delay compensation for the LWR PDE. ES control, a nonmodel-based approach for real-time optimization, is adopted to find the optimal density for the unknown fundamental diagram. A predictor feedback control design is proposed to compensate the delay effect of traffic dynamics in the freeway segment. In the end, simulation results are obtained to validate a desired performance of the controller on the nonlinear LWR model with an unknown fundamental diagram. [DOI: 10.1115/1.4048781]

1 Introduction

When there are uphills, curvature or lane-drop further downstream on freeway, a bottleneck with capacity drop appears, leading to a reduction of the total discharging flow rate from the bottleneck area and delay of travel time for the upstream traffic. Traffic congestion then forms upstream of the bottleneck as the upstream demand increases during the peak hour [1–4].

Various models have been proposed to describe the capacity drop phenomenon of the bottleneck including the first-order traffic flow models [5], discontinuous fundamental diagram in Ref. [6], and kinematic wave model in Ref. [7], which usually assume some prior knowledge of the traffic condition at the bottleneck area. The fundamental diagram of the bottleneck area is incorporated with the upstream traffic dynamics, which has been modeled with the Lighthill–Whitham–Richards (LWR) model, a first-order macroscopic partial differential equation (PDE) in Ref. [8], the cell transmission model in Ref. [2], and the link queue model [3]. In this paper, we consider a freeway segment with a bottleneck located at the outlet where the road capacity drops in the bottleneck area. The traffic flow is conserved through the bottleneck. We adopt the LWR-based model proposed in Ref. [9] due to its simplicity and conciseness in capturing the capacity drop mechanism. The density and traffic flow relation at the bottleneck area are usually hard to obtain or estimate accurately considering the uncertainty and complexity of traffic conditions. Therefore, we assume the fundamental diagram of the bottleneck area is unknown. Without knowing the flow rate and density relation in the bottleneck area, the control strategy is developed to regulate the upstream traffic such that the discharging flow rate at the bottleneck is maximized.

The traffic bottleneck congestion problem has been tackled by various traffic control approaches in recent years. Many studies focus on developing control strategies for ramp metering and variable speed limit (VSL) to avoid the capacity drop and to maximize the discharging flow rate at the bottleneck. Proportional-integrator local ramp metering strategy was developed by Wang et al. [10] to improve the performance of downstream mainline traffic flow when there is a distant downstream bottleneck. Control of lane-drop bottleneck by VSL was explored by Jin and Jin [3]. Authors approximated the LWR with discretized ordinary differential equation link queue model. A proportional-integrator-derivative controller is then developed for the VSL control strategy. In Ref. [2], the VSL control design was proposed to maximize the traffic flow at an active bottleneck using model predictive control approach. The density dynamics is described with the cell transmission model. The PDE boundary control of traffic with lane-drop problem was investigated by Bekiaris-Liberis and Krstic [8]. The traffic dynamics on a stretch of freeway upstream of the bottleneck area is governed by the LWR model. The predictor feedback control law is designed for the ramp metering at the inlet of the freeway so that the density at bottleneck area is regulated to a desired equilibrium. The emerging Lagrangian sensing and actuation with connected autonomous vehicles have been intensively studied in recent years [3,11–15]. The new control strategies are developed to emulate and improve the traditional ramp metering and VSL through the increased mobility and connectivity of the freeway traffic. In this work, boundary control of traffic with ramp metering and VSL in the presence of downstream bottleneck is studied.

We apply extremum seeking (ES) control, a nonmodel-based real-time adaptive control technique, in order to find the unknown optimal density at the bottleneck. The delay effect of the upstream traffic is compensated in designing ES control. ES control has been intensively studied over the recent years [16–31], especially after the theoretical work by Krstic and Wang [24] proving the convergence of cost function to a neighborhood of the optimal

[1]Correspondence author.

Contributed by the Dynamic Systems Division of ASME for publication in the Journal of Dynamic Systems, Measurement, and Control. Manuscript received April 30, 2020; final manuscript received October 2, 2020; published online October 29, 2020. Assoc. Editor: Scott Moura.

value by means of averaging analysis and singular perturbation. ES approach relies on a small periodic excitation, usually sinusoidal to disturb the parameters being tuned and the effect of the parameters is then quantified by the output of a nonlinear map. The search of the optimal value is therefore generated. Oliveira et al. [27] considered the problem of ES control in the presence of delays and proposed a predictor-based feedback for delay compensation, which is applied in this paper. The ES control algorithms has been applied to many applications including electromechanical valve actuators [32], in fuel-cell power maximization [33] and in trajectory optimization of high-degrees-of-freedom robot [34]. Despite the large number of previous work, the ES control has never been applied in traffic problem.

Our contribution lies in the following aspects: this is the first work on ES control of traffic governed by LWR PDE model in the presence of an unknown downstream bottleneck. The optimal density input at the inlet of the freeway segment is achieved by estimating the unknown nonlinear map at the outlet. ES control with delay compensation is first adapted to this traffic problem. The traffic dynamics is represented by a linearized LWR model in the theoretical analysis, but the simulation of ES control design is conducted on the nonlinear LWR model.

The outline of this paper: we introduce in Sec. 2 the LWR PDE model for the freeway segment upstream of bottleneck and describe density-flow relation at bottleneck with a nonlinear map. Section 3 presents the design of ES control with delay and stability analysis is conducted for the closed-loop system using backstepping transformation and averaging approach. In Sec. 4, simulation is performed on the nonlinear LWR PDE model and a quadratic fundamental diagram is considered. The conclusion and discussion of future work are given in the end.

2 Problem Statement

We consider a traffic congestion problem on a freeway-segment with lane-drop bottleneck downstream of the segment. The freeway segment upstream of the bottleneck and the lane-drop area are shown in Fig. 1, which illustrates the clear "Zone C" and the bottleneck "Zone B," respectively. The flow is conserved through the clear Zone C to the bottleneck Zone B. The local road capacity is changed due to the lane-drop in Zone B, which could be caused by working zone, accidents, or lane closure. To prevent the traffic in Zone B overflowing its capacity and then causing congestion in the freeway segment, we aim to find out the optimal density of Zone C that maximizes outgoing flux of Zone B. Traffic dynamics in Zone C is described with the macroscopic LWR traffic model for the aggregated values of traffic density. Due to the reduction of lanes in Zone B, the fundamental diagram for the flow and density relation usually change which leads to a capacity drop in Zone B. The control objective is to find the optimal input density at inlet of Zone C that drives the measurable output flux of Zone B to its unknown optimal value of an unknown fundamental diagram.

2.1 Lighthill–Whitham–Richards Traffic Model.

The traffic dynamics in Zone C upstream of Zone B is described with the first-order, hyperbolic LWR model. Traffic density $\rho(x,t)$ in Zone C is governed by the following nonlinear hyperbolic PDE, where $x \in [0,L]$, $t \in [0,\infty)$

$$\partial_t \rho + \partial_x(Q_C(\rho)) = 0 \tag{1}$$

The fundamental diagram of traffic flow and density function $Q_C(\rho)$ is given by $Q_C(\rho) = \rho V(\rho)$, where traffic velocity follows an equilibrium velocity–density relation $V(\rho)$. There are different models to describe the flux and density relation. A basic and popular choice is Greenshield's model for $V(\rho)$ which is given by $V(\rho) = v_f(1 - \frac{\rho}{\rho_m})$, where $v_f \in \mathbb{R}^+$ is defined as maximum velocity and $\rho_m \in \mathbb{R}^+$ is maximum density for Zone C. Then the fundamental diagram of flow and density function $Q_C(\rho)$ is in a quadratic form of density

$$Q_C(\rho) = -\frac{v_f}{\rho_m}\rho^2 + v_f\rho \tag{2}$$

A critical value of density segregates the traffic into the free flow regime whose density is smaller than the critical value and the congested regime whose density is greater than the critical value. The critical density is $\rho_c = \rho_m/2$ for Eq. (2). In practice, the quadratic fundamental diagram sometimes does not fit well with traffic density-flow field data. For the fundamental diagram calibrated with the freeway empirical data, the critical density usually appears at 20% of the maximum value of the density [35,36].

There are several other equilibrium models, e.g., Greenberg model, Underwood model, and diffusion model, for which the fundamental diagrams are nonlinear functions. According to Taylor expansion, second-order differentiable nonlinear function can be approximated as a quadratic function in the neighborhood of its extremum. The following assumption is made for the nonlinear fundamental diagram. The stability results derived in this paper hold locally for the general form of fundamental diagram $\mathcal{Q}(\rho)$ that satisfies the following assumption. Other density-flow models for the fundamental diagram can also be adopted $\mathcal{Q}(\rho)$ but need to satisfy Assumption 1.

ASSUMPTION 1. *The fundamental diagram $\mathcal{Q}(\rho)$ is a smooth function, and it holds $\mathcal{Q}'(\rho_c) = 0$, $\mathcal{Q}''(\rho_c) < 0$.*

Under Assumption 1, the fundamental diagram can be approximated around the critical density ρ_c as follows: $\mathcal{Q}(\rho) = q_c + \frac{\mathcal{Q}''(\rho)}{2}(\rho(t) - \rho_c)^2$, where $q_c = \mathcal{Q}(\rho_c)$ defined as the road capacity or maximum flow, with $\mathcal{Q}''(\rho) < 0$.

2.2 Lane-Drop Bottleneck Control Problem.

Due to the reduction of the number of the lanes from Zone C to Zone B, we consider the equilibrium density-flow relation of Zone B as shown in Fig. 2, as pointed out in Ref. [9]. There is a capacity drop ΔC of Q_B in Zone B compared to Q_C in Zone C after the congestion has formed upstream of the lane-drop area. The capacity drop caused by a sudden lane-drop is hard to measure in real-time and the traffic dynamics of Zone B are affected by the lane-changing and merging activities. Therefore, we assume that the fundamental diagram $Q_B(\rho)$ of Zone B is unknown. In Fig. 2, the capacity is

$$\Delta C = Q_C(\rho_c) - Q_B((1+\delta)\rho^\star) \tag{3}$$

$$q^\star = Q_C(\rho^\star) = Q_B((1+\delta)\rho^\star) \tag{4}$$

where the capacity drop ΔC is unknown. The $\rho^\star \in \mathbb{R}^+$ represents the optimal density that keeps Zone C in the free regime while $(1+\delta)\rho^\star$ reaches the critical density of Zone B so that the discharging flow rate reaches its maximum value $q^\star \in \mathbb{R}^+$. The ratio δ accounts for the density discontinuity before the outlet in Zone C and after the outlet in Zone B. We assume that ΔC and δ are unknown and therefore the optimal density and flow rate $(\rho^\star, q^\star)$ are unknown.

When there is a lane-drop bottleneck appearing downstream, the density at the outlet of Zone C is $\rho(L,t)$ governed by the PDE

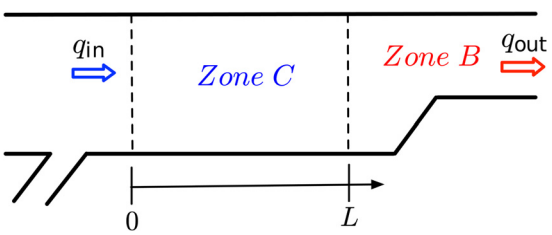

Fig. 1 Traffic on a freeway segment with lane-drop

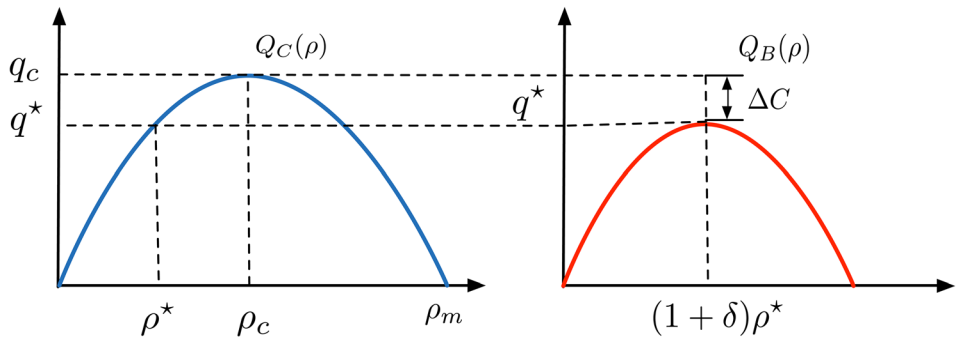

Fig. 2 Quadratic fundamental diagram for the clear Zone C and the bottleneck Zone B

in Eq. (1) for $x \in [0, L]$, $t \in [0, \infty)$. The inlet boundary flow is $q_{\text{in}}(t) = Q_C(\rho(0,t))$. The output measurement of traffic flow in Zone B, $q_{\text{out}}(t)$ is given by $Q(\rho)$ with outlet density $\rho(L,t)$, $q_{\text{out}}(t) = Q(\rho(L,t))$, where the function $Q(\rho)$ of outlet boundary $x = L$ connecting Zone C and Zone B is defined as follows:

$$Q(\rho(L,t)) = \begin{cases} Q_C(\rho(L,t)), & \rho(L,t) < \rho^\star \\ Q_C(\rho^\star) = q^\star = Q_B((1+\delta)\rho^\star), & \rho(L,t) = \rho^\star \\ Q_B((1+\delta)\rho(L,t)), & \rho(L,t) > \rho^\star \end{cases} \tag{5}$$

so that the flow is conserved through the boundary connecting Zone C to Zone B. Note that when the optimal density $\rho^\star$ is reached, the flow rate at the outlet of Zone C and the input of Zone C reaches the equilibrium and its maximum value $q^\star$.

The control objective is to design the traffic flow input $q_{\text{in}}(t)$ so that the outgoing flow in lane-drop area Zone B $q_{\text{out}}(t)$ is maximized. We aim to find out the optimal outlet density $\rho(L,t) = \rho^\star$ that maximizes $q_{\text{out}}(t)$ of Zone B and then use the LWR PDE governing the dynamics of Zone C to obtain the desirable flow input $q_{\text{in}}(t)$ from the inlet of Zone C. Here we assume that we approximate $q_{\text{out}}(t)$ with a function that satisfies Assumption 1 and $q_{\text{out}}(t)$ can be written as

$$q_{\text{out}}(t) = q^\star + \frac{H}{2}\left(\rho(L,t) - \rho^\star\right)^2 \tag{6}$$

where $H < 0$ is the unknown Hessian of the approximated static map $q_{\text{out}}(t)$.

Note that we use a static fundamental diagram to model the traffic in the bottleneck Zone B. The upstream propagating traffic waves from Zone B to Zone C cannot be captured by our model if Zone B is near bumper to bumper congestion. Since this result is focused on maximizing the discharging flow rate at the bottleneck area and the ES control seeks the optimal traffic density value in its neighborhood. In bottleneck Zone B, the closer the outlet traffic density $\rho(L,t)$ to the optimal value $\rho^\star$ where $Q'(\rho) = 0$ is satisfied, the propagating characteristic speed of the traffic waves $Q'(\rho)$ is smaller. Therefore, the spill-back traffic propogating from Zone B to Zone C is negligible in our model.

In order to find the unknown optimal density at the bottleneck area, we design ES control for the unknown static map $Q(\rho)$ with actuation dynamics governed by a nonlinear hyperbolic PDE in Eq. (1). For the control input design, we linearize the nonlinear PDE and then can represent the traffic dynamics with delay effect.

2.3 Linearized Reference Error System. We linearize the nonlinear LWR model around a constant reference density $\rho_r \in \mathbb{R}^+$, which is assumed to be close to the optimal density $\rho^\star$. Note that the reference density ρ_r is in the free regime of $Q(\rho)$ of Zone C thus is smaller than the critical density ρ_c and therefore the following is satisfied $\rho_r < \rho_c$. Define the reference error density as

$$\tilde{\rho}(x,t) = \rho(x,t) - \rho_r \tag{7}$$

and reference flux q_r is $q_r = Q(\rho_r) > 0$. By the governing Eq. (1) together with Eq. (2), the linearized reference error model is derived as

$$\partial_t \tilde{\rho}(x,t) + u\partial_x \tilde{\rho}(x,t) = 0 \tag{8}$$

$$\tilde{\rho}(0,t) = \rho(0,t) - \rho_r \tag{9}$$

where the constant transport speed u is given by $u = Q'(\rho)|_{\rho=\rho_r} = V(\rho_r) + \rho_r V'(\rho)|_{\rho=\rho_r}$. The equilibrium velocity-density relation $V(\rho)$ is a strictly decreasing function. The reference density ρ_r is in the left-half plane of the fundamental diagram $Q_c(\rho)$ which yields the following inequality for the propagation speed u, $u > 0$. We define the input density as $\varrho(t) = \rho(0,t)$, and the linearized input at inlet is

$$\tilde{\varrho}(t) = \varrho(t) - \rho_r \tag{10}$$

The linearized error dynamics in (8) and (9) is a transport PDE with an explicit solution for $t > (x/u)$ and thus is represented with input density $\tilde{\rho}(x,t) = \tilde{\varrho}(t - \frac{x}{u})$. The density variation at outlet is

$$\tilde{\rho}(L,t) = \tilde{\varrho}(t - D) \tag{11}$$

where the time delay is $D = (L/u)$. Therefore, the density at outlet is given by a delayed input density variation and the reference

$$\rho(L,t) = \rho_r + \tilde{\rho}(L,t) \tag{12}$$

Finally, substituting (11) and (12) into the static map (6), we arrive at the following:

$$\begin{aligned} q_{\text{out}}(t) &= q^\star + \frac{H}{2}\left(\tilde{\varrho}(t-D) + \rho_r - \rho^\star\right)^2 \\ &= q^\star + \frac{H}{2}\left(\varrho(t-D) - \rho^\star\right)^2 \end{aligned} \tag{13}$$

The control objective is to regulate the input $q_{\text{in}}(t)$ so that $\varrho(t-D)$ reaches to an unknown optimal $\rho^\star$ and the maximum of the uncertain quadratic flux-density map $q_{\text{out}}(t)$ can be achieved. We can apply the method of extremum seeking for static map with delays developed in Ref. [27]. The extremum seeking control is designed for finding the extremum of the unknown map.

In practice, control of density at inlet can be realized with a coordinated operation of a ramp metering and a VSL at inlet, which is widely used in freeway traffic management [37–43]. The controlled density at inlet is implemented by $\varrho(t) = (q_{\text{in}}(t)/v_c)$ where v_c is the speed limit implemented by VSL and $q_{\text{in}}(t)$ is actuated by an on-ramp metering upstream of the inlet. Note that the

linearized model is valid at the optimal density $\rho^\star$ since the reference density is assumed to be chosen near the optimal value.

3 Online Optimization by Extremum Seeking Control

In this section, we present the design of extremum seeking control with [27]. The block diagram of the delay-compensated ES algorithm applied to LWR PDE model is depicted in Fig. 3. Let $\hat{\varrho}(t)$ be the estimate of $\rho^\star$, and $e(t)$ be the estimation error defined as

$$e(t) = \hat{\varrho}(t) - \rho^\star \tag{14}$$

where $\hat{\varrho}(t)$ is an integrator of the predictor-based feedback signal $U(t)$ as $\dot{\hat{\varrho}}(t) = U(t)$. From Fig. 3, the error dynamics can be written as

$$\dot{e}(t-D) = U(t-D) \tag{15}$$

given the delayed estimation error dynamics modeled by $\epsilon(x,t) = U(t-(x/u))$. We introduce the dither signals $(M(t), N(t))$ given by

$$M(t) = \frac{2}{a}\sin(\omega t), \quad N(t) = -\frac{8}{a^2}\cos(2\omega t) \tag{16}$$

where a and ω are amplitude and frequency of a slow periodic perturbation signal $a\sin(\omega t)$ introduced later. Using the dither signals, we calculate estimates of the gradient and Hessian of the cost function, denoted as $(G(t), \hat{H}(t))$

$$G(t) = M(t)q_{\text{out}}(t), \quad \hat{H}(t) = N(t)q_{\text{out}}(t) \tag{17}$$

where $\hat{H}(t)$ is to estimate the unknown Hessian H. The averaging of $G(t)$ and $\hat{H}(t)$ yields that

$$G_{\text{av}}(t) = He_{\text{av}}(t-D), \quad \hat{H}_{\text{av}} = (Nq_{\text{out}})_{\text{av}} = H \tag{18}$$

Taking average of Eq. (15), we have $\dot{e}_{\text{av}}(t-D) = U_{\text{av}}(t-D)$, where $U_{\text{av}}(t)$ is the averaged value for $U(t)$ designed later. Substituting the above equation into Eq. (18) gives that

$$\dot{G}_{\text{av}}(t) = HU_{\text{av}}(t-D) \tag{19}$$

The motivation for predictor feedback design is to compensate for the delay by feeding back future states in the equivalent averaged system $G_{av}(t+D)$. Given an arbitrary control gain $k>0$, we aim to design

$$U_{\text{av}}(t) = kG_{\text{av}}(t+D), \quad \forall t \geq 0 \tag{20}$$

which requires knowledge of future states. Therefore, we have the following by plugging Eq. (20) into Eq. (15):

$$\dot{e}_{\text{av}}(t) = U_{\text{av}}(t) = kHe_{\text{av}}(t), \quad \forall t \geq D \tag{21}$$

Reminding that $k>0, H<0$, the equilibrium of the average system $e_{\text{av}}(t)=0$ is exponentially stable. Applying the variation of constants formula $G_{\text{av}}(t+D) = G_{\text{av}}(t) + \hat{H}_{\text{av}}(t)\int_{t-D}^{t} U_{\text{av}}(\tau)d\tau$ and, from Eq. (20), one has

$$U_{\text{av}}(t) = k(G_{\text{av}}(t) + \hat{H}_{\text{av}}(t)\int_{t-D}^{t} U_{\text{av}}(\tau)d\tau) \tag{22}$$

which represents the future state $G_{\text{av}}(t+D)$ in Eq. (19) in terms of the average control signal $U_{\text{av}}(\tau)$ for $\tau \in [t-D, t]$. The control input is infinite-dimensional due to its use of history over the past D time units.

For the stability analysis in which the averaging theorem for infinite dimensional systems is used, we employ a low-pass filter for the above basic predictor feedback controller and then derive an infinite dimensional and averaging-based predictor feedback given by

$$U(t) = \mathscr{T}\{k(G(t) + \hat{H}(t)\int_{t-D}^{t} U(\tau)d\tau)\} \tag{23}$$

where $k>0$ is an arbitrary control gain, and the Hessian estimate $\hat{H}(t)$ is updated according to Eq. (17), satisfying average property in Eq. (18). $\mathscr{T}\{\}$ is the low pass filter operator defined by

$$\mathscr{T}\{\varphi(t)\} = \mathscr{L}^{-1}\left\{\frac{c}{s+c}\right\} * \varphi(t) \tag{24}$$

where $c \in \mathbb{R}^+$ is the corner frequency, $\mathscr{L}^{-1}$ is the inverse Laplace transformation, and $*$ is the convolution in time.

THEOREM 1. *Consider the closed-loop system in Fig. 3. There exsit $c_0>0$ such that $\forall c \geq c_0$, and $\omega_0(c_0)>0$ such that $\forall \omega > \omega_0$, the closed-loop system has a unique exponentially stable periodic solution in period $T = (2\pi/\omega)$, denoted by $e^T(t-D), U^T(\tau), \forall \tau \in [t-D, t]$, satisfying $\forall t > 0$*

$$\left(|e^T(t-D)|^2 + |U^T(t)|^2 + \int_0^D |U^T(\tau)|^2 d\tau\right)^{\frac{1}{2}} \leq \mathcal{O}(1/\omega) \tag{25}$$

Furthermore

$$\lim_{t\to+\infty} \sup|\varrho(t) - \rho^\star| = \mathcal{O}(a + 1/\omega) \tag{26}$$

$$\lim_{t\to+\infty} \sup|q_{\text{out}}(t) - q^\star| = \mathcal{O}(a^2 + 1/\omega^2) \tag{27}$$

The detailed proof of Theorem 1 is carried out in the Appendix, following Ref. [27]. First, we show the exponential stability of the average error-dynamics system using a backstepping

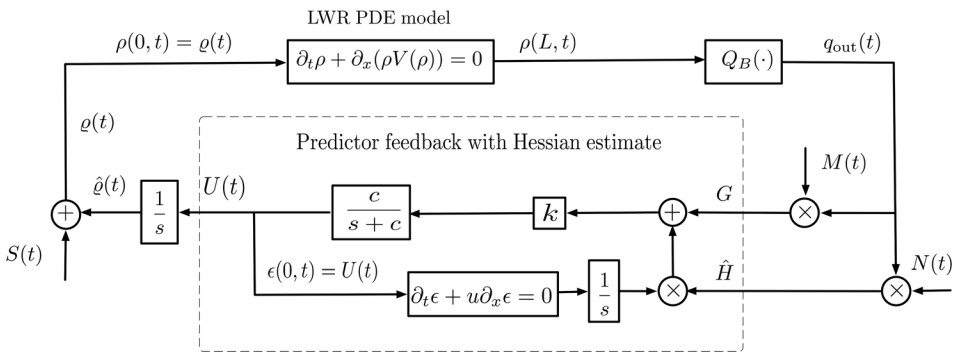

Fig. 3 Block diagram for implementation of ES control design for nonlinear LWR PDE model

transformation. Then the averaging theorem for infinite-dimensional systems [44] is invoked to show the exponential stability of the original error-dynamics system (A4)–(A6). Using Lyapunov analysis, we show the convergence of $(\varrho(t), q_{\text{out}}(t))$ to a neighborhood of the extremum $(\rho^\star, q^\star)$.

4 Simulation Result

In simulation, we choose Greenshield's model for equilibrium velocity–density relation. For the clear section Zone C, the fundamental diagram of traffic flow-density relation is given by $Q(\rho) = -(v_f/\rho_m)\rho^2 + v_f\rho$. We choose our model parameters based on the data-fitted LWR model in Ref. [36]. The maximum density is chosen to be $\rho_m = 6\,\text{lanes}/7.5\,\text{m} = 0.8\,\text{veh/m} = 800\,\text{veh/km}$, where the 7.5 m equals to the average vehicle length 5 m plus 50% safety distance. The maximum velocity is $v_f = 16.7\,\text{m/s} = 60\,\text{km/h}$. This $Q(\rho)$ is used in the nonlinear LWR PDE model simulation which describes the traffic dynamics upstream of bottleneck area. The maximum output flow also known as road capacity of Zone C is $q_c = \max_{0\le\rho\le\rho_m} Q(\rho) = 3.2\,\text{veh/s} = 1920\,\text{veh/h/lane}$. The length of freeway segment is $L = 100\,\text{m}$. If we consider a linearized LWR for Zone C, the characteristic speed is $u = Q_c'(\rho)|_{\rho=\rho_r=0.2\,\text{veh/m}} = 8.4\,\text{m/s}$. The time delay for input to reach the bottleneck area is $D = L/u = 12\,\text{s}$.

The fundamental diagram in the bottleneck area $Q_B(\rho)$, optimal/critical density $\rho^\star$, and maximum output flow $q^\star$ are assumed to be unknown when there is sudden lane-closure due to an accident or a lane closure. The following function and parameters are chosen for simulation purpose. For the bottleneck section Zone B, we consider the situation that only four out of six lanes still function. As a result, the road capacity reduces and we define the capacity reduction rate as $C_d = 40\%$ compared with Zone C. The outgoing flow $q_{\text{out}}(t) = Q(\rho(L,t))$ of the bottleneck area is approximated with

$$q_{\text{out}}(t) = q^\star + \frac{H}{2}\left(\varrho(t-D) - \rho^\star\right)^2 \tag{28}$$

where $\varrho_m = 0.48\,\text{vehicles/m}$ is the maximum density for reduced lanes in the bottleneck area and the same maximum velocity v_f is considered. The optimal/critical density $\rho^\star$ and maximum output flow $q^\star$ are

$$\rho^\star = \frac{1}{2}\varrho_m = 0.24\,\text{veh/m} \tag{29}$$

$$q^\star = (1-\Delta C)q_c = 1.92\,\text{veh/s} \tag{30}$$

Compared with the capacity of Zone C q_c, there is a capacity drop ΔC for optimal flow rate $q^\star$ of the bottleneck area. The Hessian is obtained by taking second derivative of $q_{\text{out}}(t)$

$$H = -\frac{2v_f}{\varrho_m} = -69.5 \tag{31}$$

The Godnov scheme is employed for simulation of nonlinear LWR PDE model. The method is derived from the solution of local Riemann problems. The road segment is divided into spatial cell Δx and the solution is advanced in time-step Δt, which satisfy the following Courant–Friedrichs–Lewy condition $u_{\max}\frac{\Delta t}{\Delta x} < 1$, where $u_{\max}$ is the maximum characteristic speed. We choose the spatial cell $\Delta x = 0.05\,\text{m}$ sufficiently small so that numerical errors are negligibly small relative to the errors of the model.

The simulation result of the closed-loop system with ES control is shown in Figs. 4–7. The parameters of the sinusoidal input and the designed controller are chosen to be $\omega = 2.75\pi$, $a = 0.05, c = 50, K = 0.005$. The adaptation gain is k, while a and ω are used in the computation of the frequencies and amplitudes for the perturbation signals $M(t), N(t)$ in Eq. (16) and $S(t)$ in Eq. (A2). The speed of convergence and the ultimate residual sets of the ES algorithm are influenced by the values of k, a, and ω.

The evolution of the density PDE state $\rho(x,t)$ modeled by the LWR model (1) is shown in Fig. 4. The inlet density boundary input and outlet boundary values and the intial conditionare highlighted. One can observe that density value $\rho(L,t)$ in Fig. 5 converges to a neighborhood of the optimal value $\rho^\star = 0.24\,\text{veh/m}$ and the output flow of the bottleneck in Fig. 6 converges to a neighborhood of the extremum point $q^\star = 1.92\,\text{veh/s}$. The Hessian estimate converges to the prescribed value -69.5 in Fig. 7. The convergence to optimal values is achieved in 40 s. In contrast, if we do not employ ES control for input density and the incoming flow depends only on upstream traffic. The open-loop system is shown in Fig. 8. The evolution of outgoing flow at the bottleneck area is run for 150 s. The outgoing flow of the bottleneck area keeps decreasing and therefore congestion at the bottleneck area is getting worse till a bumper-to-bumper jam as shown in Fig. 9.

As mentioned in the stability analysis of Sec. 4, the performance of the proposed ES is guaranteed only locally, i.e., the initial density state must be sufficiently close to the optimal density. We investigate how far the initial density can be from the optimal density by trying some initial density profiles. In particular, first we investigate the simulation with the initial density profile as a uniform distribution, namely

$$\rho(x,0) = \rho_0, \quad \forall x \in [0,L] \tag{32}$$

where $\rho_0 \in (0,\rho_c)$ for the traffic in Zone C to be free regime in the fundamental diagram. Through trying several values for $\rho_0 \in (0,\rho_c)$ in simulations, we observe that the convergence of the output density to the optimal density is achieved for the range of $\rho_0 \in (\rho_l,\rho_h)$, where $\rho_l = 0.16\,\text{veh/m}$ and $\rho_h = 0.24\,\text{veh/m}$.

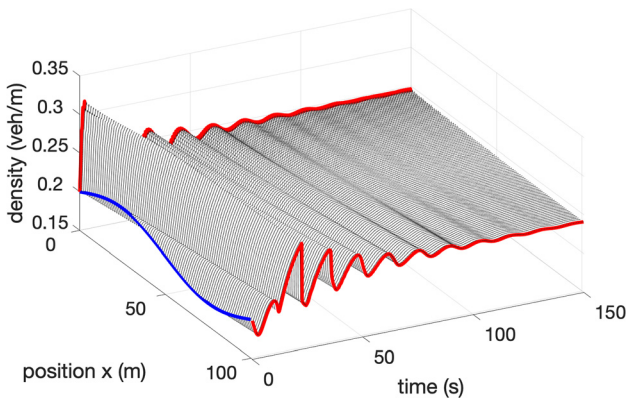

Fig. 4 Traffic density state evolution $\rho(x,t)$ of nonlinear LWR model in Zone C

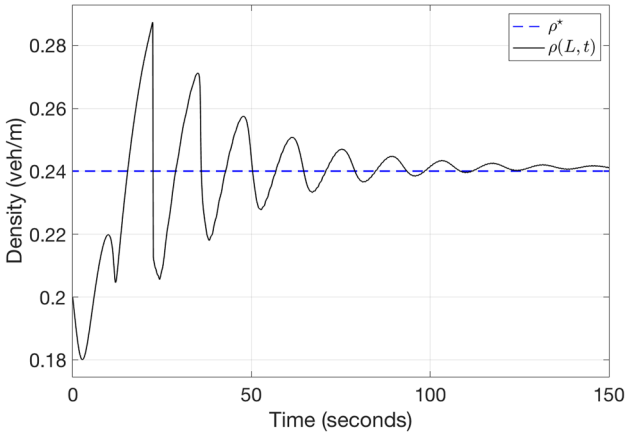

Fig. 5 Traffic density $\rho(L,t)$ at the outlet of Zone C by nonlinear LWR model which is the input density for bottleneck area

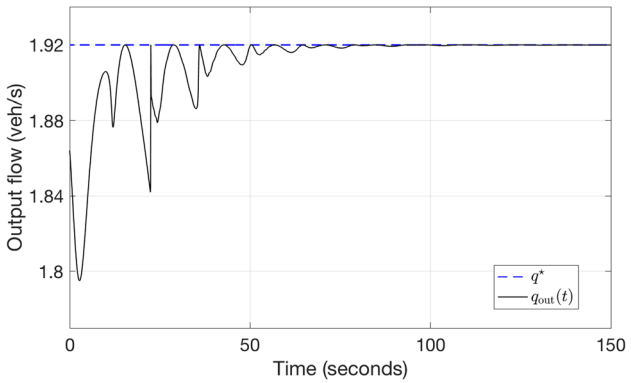

Fig. 6 Outgoing traffic flow of the bottleneck area $q_{\text{out}}(t)$ which is also the output flow for bottleneck area and the optimal value of outgoing flow $q^\star$

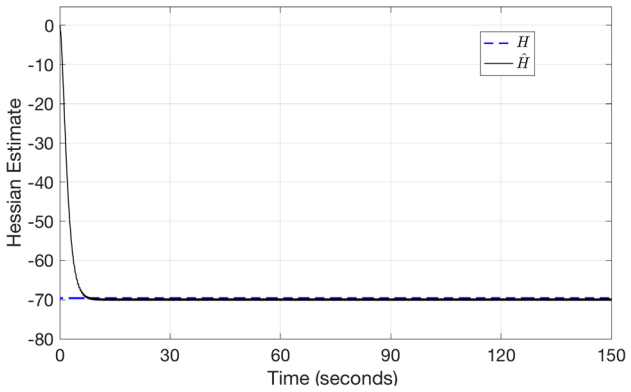

Fig. 7 Hessian estimate $\hat{H}(t)$ of the ES control and prescribed Hessian value H

Compared with the initial reference density we use $\rho_r = 0.2\,\text{veh/m}$, the range of variation is $\pm 20\%$. In the following, we show the converegence results for an initial density profiel that reaches both the upper and lower limits shown in Fig. 9.

We set a "soft shockwave" in Fig. 9, given by

$$\rho(x,0) = \frac{\rho_h - \rho_l}{2}\sin\left(\frac{\pi}{L}x - \frac{\pi}{2}\right) + \frac{\rho_h + \rho_l}{2} \tag{33}$$

where $0 < \rho_l < \rho_h < \rho_c$. Note that the soft shock function defined above is a smooth and monotonically increasing function satisfying $\rho(0,0) = \rho_l$ and $\rho(L,0) = \rho_h$. We investigate the simulation

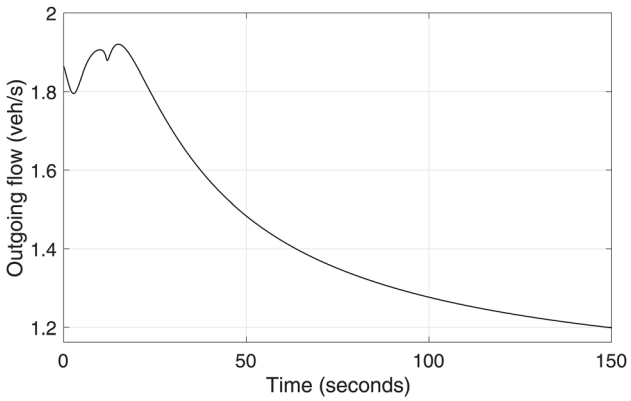

Fig. 8 Output traffic flow of the bottleneck area without ES Control

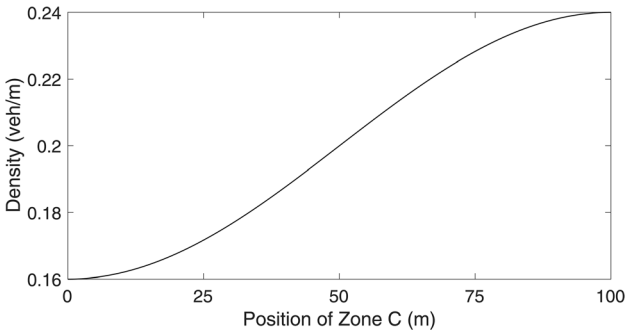

Fig. 9 The shape of the density initial profile for Zone C is a soft shockwave with higher density near the bottleneck and lower density closer to the inlet of the Zone C

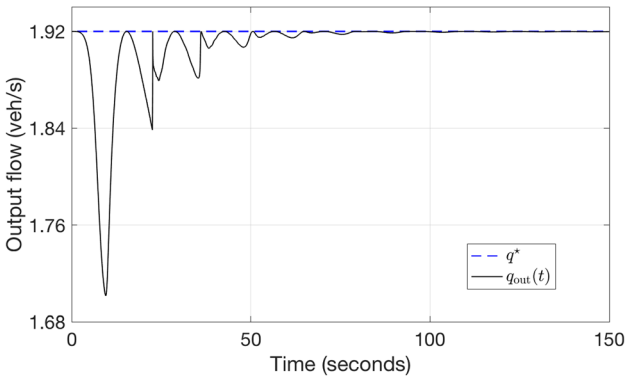

Fig. 10 The evolution of the outgoing traffic flow of the bottleneck area $q_{\text{out}}(t)$ for the soft-shockwave initial density profile

results through varying the parameters (ρ_l, ρ_h) satisfying $0 < \rho_l < \rho_h < \rho_c$. Such a sensitivity of initial condition can be regarded as a domain of attraction under specific condition. In Figs. 10 and 11, we show the convergence results of the input density and the outgoing flow when $\rho_l = 0.16\,\text{veh/m}$ and $\rho_h = 0.24\,\text{veh/m}$. These results illustrate a relatively large sensitivity of initial condition, which validates the performance of the proposed ES control for the lane-drop traffic model we consider. While it is difficult to survey the domain of attraction rigorously, semiglobal convergence could be guaranteed by adapting the amplitude of the dither signals [29], and nearly a global stability could be also achieved by choosing tuning parameters as time-varying [45].

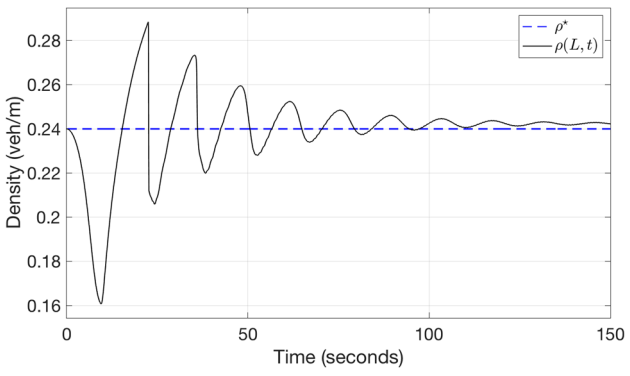

Fig. 11 The evolution of the traffic density $\rho(L,t)$ for the soft-shockwave initial density profile

5 Conclusion

In this paper, we employ ES control to find an optimal density input for freeway traffic when there is a downstream bottleneck. To prevent traffic flow in bottleneck area overflowing the road capacity and furthermore causing congestion upstream in the freeway segment, the incoming traffic density at inlet of the freeway segment is regulated. The control design is achieved with delay compensation for ES control considering the upstream traffic is governed by the linearized LWR model. The optimal density and flow are achieved in the bottleneck area. The theoretical result is validated in simulation with the control design being applied to the nonlinear LWR PDE model along with an unknown fundamental diagram.

For future work, multiple distinct delays existing in the multilanes are going to be considered when regulating the distant downstream traffic bottleneck. It would also be interesting for authors to develop ES control with bounded update rates [46] under input delays exhibited through the LWR model and to develop a stochastic version of the algorithm presented in the paper by applying the results from Refs. [25] and [28]. To further demonstrate the impact of this work for traffic application and understand how the proposed extremum seeking controller works in practice, it is of research interest to validate this result with traffic field data [47] and test it with microscopic simulator.

Acknowledgment

The third author would like to thank the Brazilian funding agencies CNPq, CAPES, and FAPERJ for the financial support.

Appendix: Proof of Theorem 1

The proof Theorem 1 is carried out through the following steps.

A.1 Closed-Loop System. The estimate $\hat{\varrho}(t)$ of the unknown optimal outgoing $\rho^\star$ is an integrator of the predictor-based feedback signal $U(t)$ as $\dot{\hat{\varrho}}(t) = U(t)$, and it follows that $\dot{e}(t-D) = U(t-D)$. The input $\varrho(t)$ to LWR PDE model is given by

$$\varrho(t) = \hat{\varrho}(t) + S(t) \tag{A1}$$

where the dither signal $S(t)$ is the inverse operator of a delayed perturbation signal $a\sin(\omega t)$, described as

$$S(t) = a\sin(\omega(t+D)) \tag{A2}$$

Substituting $S(t)$ into Eq. (A1), we have

$$\varrho(t) = \hat{\varrho}(t) + a\sin(\omega(t+D)) \tag{A3}$$

The delayed estimation error dynamics can be written as transport PDE system, $x \in [0, L]$

$$\dot{e}(t-D) = \epsilon(L,t) \tag{A4}$$

$$\partial_t \epsilon(x,t) = -u\partial_x \epsilon(x,t) \tag{A5}$$

$$\epsilon(0,t) = U(t) \tag{A6}$$

where it is straightforward to obtain that $\epsilon(x,t) = U(t-(x/u))$. Combining Eqs. (13) and (14), the relation among the estimation error $e(t)$, the input density $\varrho(t)$, and optimal outlet density $\rho^\star$ is given by

$$e(t) + a\sin(\omega t) = \varrho(t) - \rho^\star \tag{A7}$$

Substituting the above relation into the output map in Eq. (13), we obtain the following equation:

$$q_{\text{out}}(t) = q^\star + \frac{H}{2}\left(e(t-D) + a\sin(\omega t)\right)^2 \tag{A8}$$

Plugging $M(t)$ and $G(t)$ into Eq. (17) and representing the delayed input with PDE state $\epsilon(x,t)$, we have

$$U(t) = \mathscr{T}\{k(G(t) + \hat{H}(t)\int_0^L \epsilon(\tau,t)d\tau)\} \tag{A9}$$

$$G(t) = \frac{2}{a}\sin(\omega t)q_{\text{out}}(t) \tag{A10}$$

$$\hat{H}(t) = -\frac{8}{a^2}\cos(2\omega t)q_{\text{out}}(t) \tag{A11}$$

It yields

$$U(t) = \mathscr{T}\left\{kq_{\text{out}}(t)\left(\frac{2}{a}\sin(\omega t) - \frac{8}{a^2}\cos(2\omega t)\int_0^L \epsilon(\tau,t)d\tau\right)\right\} \tag{A12}$$

and by substituting q_{out} with Eq. (A8) and combining with transport PDE in Eqs. (A4)–(A6), we can write the closed-loop system as

$$\dot{e}(t-D) = \epsilon(L,t) \tag{A13}$$

$$\partial_t \epsilon(x,t) = -u\partial_x \epsilon(x,t) \tag{A14}$$

$$\epsilon(0,t) = \mathscr{T}\left\{k\left(q^\star + \frac{H}{2}\left(e(t-D) + a\sin(\omega t)\right)^2\right)\left(\frac{2}{a}\sin(\omega t) - \frac{8}{a^2}\cos(2\omega t)\int_0^L \epsilon(\tau,t)d\tau\right)\right\} \tag{A15}$$

A.2 Average System. Expanding Eq. (A15) and taking average of the closed-loop system, we obtain average model by setting the averages of sine and cosine functions of $n\omega$, $(n = 1, 2, 3, 4)$ to zeros. Note that the averaged controller satisfies

$$\dot{U}_{av}(t) + cU_{av}(t) = ck(G_{av}(t) + H\int_0^L \epsilon_{\text{av}}(\tau,t)d\tau) \tag{A16}$$

where $c > 0$ is the corner frequency of the low pass filter and $k > 0$ is the control gain. Denoting

$$\theta(t) = e(t-D) \tag{A17}$$

the average system of (A13)–(A15) is rewritten by

$$\dot{\theta}_{\text{av}}(t) = \epsilon_{\text{av}}(L,t) \tag{A18}$$

$$\partial_t \epsilon_{\text{av}}(x,t) = -u\partial_x \epsilon_{\text{av}}(x,t) \tag{A19}$$

$$\partial_t \epsilon_{\text{av}}(0,t) = -c\epsilon_{\text{av}}(0,t) + ckH(\theta_{\text{av}}(t) + \int_0^L \epsilon_{\text{av}}(\tau,t)d\tau) \tag{A20}$$

A.3 Backstepping Transformation. We apply backstepping transformation [48] for the averaged delay state

$$w(x,t) = \epsilon_{\text{av}}(x,t) - kH[\theta_{\text{av}}(t) + \int_x^L \epsilon_{\text{av}}(\tau,t)d\tau] \tag{A21}$$

where $k > 0$ and $H < 0$. The average system is mapped into the target system

$$\dot{\theta}_{\text{av}}(t) = kH\theta_{\text{av}}(t) + w(L,t) \tag{A22}$$

$$\partial_t w(x,t) = -u\partial_x w(x,t) \tag{A23}$$

$$\partial_t w(0,t) = -(c+kH)w(0,t) - (kH)^2\left[e^{\frac{kHL}{u}}\theta_{\text{av}}(t) + \int_0^L e^{\frac{kH(L-\tau)}{u}} w(\tau,t)d\tau\right] \tag{A24}$$

Combining Eqs. (A20) and (A21), we have $w(0,t) = -(1/c)\partial_t \epsilon_{\text{av}}(0,t)$. Taking time derivative on Eq. (A21) for $w(0,t)$, we obtain

$$\partial_t w(0,t) = \partial_t \epsilon_{\text{av}}(0,t) - kH\epsilon_{\text{av}}(0,t) \tag{A25}$$

The inverse transformation is given by

$$\epsilon_{\text{av}}(x,t) = w(x,t) + kH\left[e^{\frac{kH(L-x)}{u}}\theta_{\text{av}}(t) + \int_x^L e^{\frac{kH(L-x+\tau)}{u}}\epsilon_{\text{av}}(\tau,t)d\tau\right] \tag{A26}$$

Plugging Eqs. (A26) and (A20) into Eq. (A25), we obtain Eq. (A24) in the target system.

A.4 Lyapunov Functional. Now consider the following Lyapunov functional for the target system

$$V(t) = \frac{a\theta_{\text{av}}^2(t)}{2} + \int_0^L e^{-x}w^2(x,t)dx + \frac{1}{2}w^2(0,t) \tag{A27}$$

where the parameter $a > 0$ is chosen later. Taking time derivative of the Lyapunov function, we have

$$\begin{aligned}\dot{V}(t) \le{}& akH\theta_{\text{av}}^2 + \frac{a}{2b}\theta_{\text{av}}^2 + \left(\frac{ab - ue^{-L}}{2}\right)w^2(L,t)\\ &-\frac{u}{2}\int_0^L e^{-x}w^2(x,t)dx + w(0,t)\left(w_t(0,t) + \frac{u}{2}w(0,t)\right)\end{aligned} \tag{A28}$$

where the positive constant b satisfies the following, $b = (ue^{-L}/a)$ so that $ab - ue^{-L} = 0$. The positive constant a is chosen as $a = -ukHe^{-L}$. Substituting $w_t(0,t)$ by Eq. (A24) and using Young's, Cauchy–Schwarz inequalities, the last term in Eq. (A28) is bounded by

$$\begin{aligned}&w(0,t)\left(w_t(0,t) + \frac{u}{2}w(0,t)\right)\\ &\le -\left(c - \frac{u}{2} + kH\right)w^2(0,t)\\ &+\frac{e^L a^2}{4u}\theta_{\text{av}}^2(t) + \frac{ue^{-L}}{a^2}\left|(kH)^2 e^{\frac{kHL}{u}}\right|^2 w(0,t)^2\\ &+\frac{ue^{-L}}{4}||w(t)||^2 + \frac{e^L}{u}\left\|(kH)^2 e^{\frac{kH(L-\tau)}{u}}\right\|^2 w(0,t)^2\end{aligned} \tag{A29}$$

Plugging Eq. (A29) into Eq. (A28), one can arrive at

$$\begin{aligned}\dot{V}(t) \le{}& -\frac{e^L a^2}{4u}\theta_{\text{av}}^2(t) - \frac{ue^{-L}}{4}\int_0^L w^2(x,t)dx\\ &-(c - c_0)w^2(0,t)\end{aligned} \tag{A30}$$

where c_0 is defined as $c_0 = \frac{u}{2} - kH + \frac{ue^{-L}}{a^2}\left|(kH)^2 e^{\frac{kHL}{u}}\right|^2 + \frac{e^L}{u}\left|\left|(kH)^2 e^{\frac{kH(L-\tau)}{u}}\right|\right|^2$ where $\tau \in [0,L]$. An upper bound for c_0 can be obtained from lower and upper bounds of the unknown Hessian H. Therefore, by choosing c such that $c > c^*$, we obtain

$$\dot{V}(t) \le -\mu V(t) \tag{A31}$$

for some $\mu > 0$. Thus, the closed-loop system is exponentially stable in the sense of the L^2 norm $(|\theta_{\text{av}}(t)|^2 + \int_0^L w^2(x,t)dx + w^2(0,t))^{1/2}$. By the invertibility of the transformation, we can see that there exist constants α_1 and α_2 such that the following inequality is obtained

$$\alpha_1\Psi(t) \le V(t) \le \alpha_2\Psi(t) \tag{A32}$$

where $\Psi(t) \triangleq |\theta_{\text{av}}(t)|^2 + \int_0^L \epsilon_{\text{av}}^2(x,t)dx + \epsilon_{\text{av}}^2(L,t)$, or equivalently

$$\Psi(t) \triangleq |\theta_{\text{av}}(t-D)|^2 + \int_{t-D}^t U_{\text{av}}^2(\tau)d\tau + U_{\text{av}}^2(t) \tag{A33}$$

Hence, with Eq. (A31), we get

$$\Psi(t) \le \frac{\alpha_2}{\alpha_1}e^{-\mu t}\Psi(0) \tag{A34}$$

which completes the proof of exponential stability of the averaged system.

A.5 Averaging Theorem. The closed-loop system is written as

$$\dot{e}(t-D) = U(t-D) \tag{A35}$$

$$\dot{U}(t) = -cU(t) + c\{k(G(t) + \hat{H}(t)\int_{t-D}^t U(\tau)d\tau)\} \tag{A36}$$

Defining the state vector $z(t)$ as $z(t) = [e(t-D), U(t)]^T$, and noting that $\int_{t-D}^t U(\tau)d\tau = \int_{-D}^0 U(t+\tau)d\tau$, we can write the dynamics of z as a functional differential equation described by $\dot{z}(t) = f(\omega t, z_t)$, where $z_t(\tau) = z(t+\tau)$ for $-D \le \tau \le 0$. According to Eq. (A34), the origin of the average closed-loop system with transport PDE is exponentially stable. Applying the averaging theorem for infinite dimensional systems developed in Ref. [44], for ω sufficiently large, Eqs. (A13)–(A15) has a unique exponentially stable periodic solution around its equilibrium satisfying (25).

A.6 Asymptotic Convergence to a Neighborhood of the Extremum $(\rho^\star, q^\star)$. By using the change of variables (A17) and then integrating both sides of Eq. (A13) within the interval $[t, \sigma + D]$, we have

$$\theta(\sigma + D) = \theta(t) + \int_t^{\sigma+D} \epsilon(L,s)ds \tag{A37}$$

From (A.1), we can rewrite (A37) in terms of U, namely

$$\theta(\sigma + D) = \theta(t) + \int_{t-D}^{\sigma} U(\tau)d\tau \tag{A38}$$

We define $\vartheta(\sigma) = \theta(\sigma + D)\,, \quad \forall\sigma \in [t-D, t]\,.$ Applying Eq. (A38) to the above equation, we get

$$\vartheta(\sigma) = \vartheta(t-D) + \int_{t-D}^{\sigma} U(\tau)d\tau\,, \quad \forall\sigma \in [t-D, t] \tag{A39}$$

By applying the supremum norm in both sides of Eq. (A39) and using Cauchy–Schwarz inequality, we have

$$\sup_{t-D\le\sigma\le t}|\vartheta(\sigma)| = \sup_{t-D\le\sigma\le t}|\vartheta(t-D)| + \sup_{t-D\le\sigma\le t}\left|\int_{t-D}^{\sigma}U(\tau)d\tau\right|$$
$$\le |\vartheta(t-D)| + \sqrt{D}\left(\int_{t-D}^{t}U^2(\tau)d\tau\right)^{1/2}$$
$$\le (1+\sqrt{D})(|\vartheta(t-D)|^2 + \int_{t-D}^{t}U^2(\tau)d\tau)^{1/2} \tag{A40}$$

From Eq. (A40), it is straightforward to conclude that

$$\sup_{t-D\le\sigma\le t}|\vartheta(\sigma)| \le (1+\sqrt{D})(|\vartheta(t-D)|^2 + \int_{t-D}^{t}U^2(\tau)d\tau)^{1/2} \tag{A41}$$

and thus

$$|\vartheta(t)| \le (1+\sqrt{D})(|\tilde{\theta}(t-D)|^2 + \int_{t-D}^{t}U^2(\tau)d\tau)^{1/2} \tag{A42}$$

The above inequality (A42) can be given in terms of the periodic solution $\vartheta^{\Pi}(t-D)$, $U^{\Pi}(\sigma)$, $\forall\sigma\in[t-D,t]$ as follows:

$$|\vartheta(t)| \le (1+\sqrt{D})(|\vartheta(t-D)-\vartheta^{\Pi}(t-D)+\vartheta^{\Pi}(t-D)|^2$$
$$+\int_{t-D}^{t}[U(\tau)-U^{\Pi}(\tau)+U^{\Pi}(\tau)]^2d\tau)^{1/2} \tag{A43}$$

Applying Young's inequality, the right-hand side of Eq. (A43) and $|\vartheta(t)|$ can be majorized by

$$|\vartheta(t)| \le \sqrt{2}\,(1+\sqrt{D})(|\vartheta(t-D)-\vartheta^{\Pi}(t-D)|^2 + |\vartheta^{\Pi}(t-D)|^2$$
$$+\int_{t-D}^{t}[U(\tau)-U^{\Pi}(\tau)]^2d\tau + \int_{t-D}^{t}[U^{\Pi}(\tau)]^2d\tau)^{1/2} \tag{A44}$$

From the averaging theorem [44], we have the exponential convergence

$$\vartheta(t-D)-\vartheta^{\Pi}(t-D)\to 0 \tag{A45}$$

$$\int_{t-D}^{t}[U(\tau)-U^{\Pi}(\tau)]^2d\tau\to 0 \tag{A46}$$

Hence

$$\limsup_{t\to+\infty}|\vartheta(t)| = \sqrt{2}\,(1+\sqrt{D})$$
$$\times\left(|\vartheta^{\Pi}(t-D)|^2 + \int_{t-D}^{t}[U^{\Pi}(\tau)]^2d\tau\right)^{1/2} \tag{A47}$$

From Eqs. (25) and (A47), we can write

$$\limsup_{t\to+\infty}|\vartheta(t)| = \mathcal{O}(1/\omega) \tag{A48}$$

From Eq. (14) and recalling that $\varrho(t)=\hat{\rho}(t)+a\sin(\omega(t+D))$ and $\theta(t)=e(t-D)$, one has that

$$\varrho(t)-\rho^{\star} = \vartheta(t)+a\sin(\omega(t+D)) \tag{A49}$$

Since the first term in the right-hand side of Eq. (A49) is ultimately of order $\mathcal{O}(1/\omega)$ and the second term is of order $\mathcal{O}(a)$, then

$$\limsup_{t\to+\infty}|\varrho(t)-\rho^{\star}| = \mathcal{O}(a+1/\omega) \tag{A50}$$

Finally, from Eq. (13), we get Eq. (27) and the proof is complete.

References

[1] Chung, K., Rudjanakanoknad, J., and Cassidy, M. J., 2007, "Relation Between Traffic Density and Capacity Drop at Three Freeway Bottlenecks," Transp. Res. Part B, **41**(1), pp. 82–95.
[2] Hadiuzzaman, M., Qiu, T. Z., and Lu, X. Y., 2013, "Variable Speed Limit Control Design for Relieving Congestion Caused by Active Bottlenecks," J. Transp. Eng., **139**(4), pp. 358–370.
[3] Jin, H. Y., and Jin, W. L., 2015, "Control of a Lane-Drop Bottleneck Through Variable Speed Limits," Transp. Res. Part C, **58**, pp. 568–584.
[4] Kim, K., and Cassidy, M. J., 2012, "A Capacity-Increasing Mechanism in Freeway Traffic," Transp. Res. Part B, **46**(9), pp. 1260–1272.
[5] Kontorinaki, M., Spiliopoulou, A., Roncoli, C., and Papageorgiou, M., 2017, "First-Order Traffic Flow Models Incorporating Capacity Drop: Overview and Real-Data Validation," Transp. Res. Part B, **106**, pp. 52–75.
[6] Lu, Y., Wong, S. C., Zhang, M., and Shu, C. W., 2009, "The Entropy Solutions for the Lighthill-Whitham-Richards Traffic Flow Model With a Discontinuous Flow-Density Relationship," Transp. Sci., **43**(4), pp. 511–530.
[7] Jin, W. L., 2013, "A Multi-Commodity Lighthill-Whitham-Richards Model of Lane-Changing Traffic Flow," Procedia-Soc. Behav. Sci., **80**, pp. 658–677.
[8] Bekiaris-Liberis, N., and Krstic, M., 2018, "Compensation of Actuator Dynamics Governed by Quasilinear Hyperbolic PDEs," Automatica, **92**, pp. 29–40.
[9] Treiber, M., and Kesting, A., 2013, "Traffic flow dynamics," *Traffic Flow Dynamics: Data, Models and Simulation*, Springer-Verlag, Berlin.
[10] Wang, Y., Kosmatopoulos, E. B., Papageorgiou, M., and Papamichail, I., 2014, "Local Ramp Metering in the Presence of a Distant Downstream Bottleneck: Theoretical Analysis and Simulation Study," IEEE Trans. Intell. Transp. Syst., **15**(5), pp. 2024–2039.
[11] Čičić, M., and Johansson, K. H., 2018, "Traffic Regulation Via Individually Controlled Automated Vehicles: A Cell Transmission Model Approach," 21st International Conference on Intelligent Transportation Systems (ITSC), Maui, HI, Nov. 4–7, pp. 766–771.
[12] Delle Monache, M. L., and Goatin, P., 2014, "Scalar Conservation Laws With Moving Constraints Arising in Traffic Flow Modeling: An Existence Result," J. Differ. Equations, **257**(11), pp. 4015–4029.
[13] Lattanzio, C., Maurizi, A., and Piccoli, B., 2011, "Moving Bottlenecks in Car Traffic Flow: A PDE-ODE Coupled Model," SIAM J. Math. Anal., **43**(1), pp. 50–67.
[14] Piacentini, G., Goatin, P., and Ferrara, A., 2018, "Traffic Control Via Moving Bottleneck of Coordinated Vehicles," IFAC-PapersOnLine, **51**(9), pp. 13–18.
[15] Villa, S., Goatin, P., and Chalons, C., 2017, "Moving Bottlenecks for the Aw-Rascle-Zhang Traffic Flow Model," Discrete Contin. Dyn. Syst.-B, **22**(10), pp. 3921–3952.
[16] Ariyur, K. B., and Krstic, M., 2003, *Real-Time Optimization by Extremum-Seeking Control*, Wiley, USA.
[17] Benosman, M., 2016, *Learning-Based Adaptive Control: An Extremum Seeking Approach–Theory and Applications*, Butterworth-Heinemann, United Kingdom.
[18] Feiling, J., Koga, S., Krstic, M., and Oliveira, T. R., 2018, "Gradient Extremum Seeking for Static Maps With Actuation Dynamics Governed by Diffusion PDEs," Automatica, **95**, pp. 197–206.
[19] Ghaffari, A., Krstic, M., and Nesic, D., 2012, "Multivariable Newton-Based Extremum Seeking," Automatica, **48**(8), pp. 1759–1767.
[20] Ghaffari, A., Krstic, M., and Seshagiri, S., 2014, "Power Optimization and Control in Wind Energy Conversion Systems Using Extremum Seeking," IEEE Trans. Control Syst. Technol., **22**(5), pp. 1684–1695.
[21] Ghaffari, A., Krstic, M., and Seshagiri, S., 2014, "Power Optimization for Photovoltaic Microconverters Using Multivariable Newton-Based Extremum Seeking," IEEE Trans. Control Syst. Technol., **22**(6), pp. 2141–2149.
[22] Guay, M., and Zhang, T., 2003, "Adaptive Extremum Seeking Control of Nonlinear Dynamic Systems With Parametric Uncertainties," Automatica, **39**(7), pp. 1283–1293.
[23] Krstic, M., 2000, "Performance Improvement and Limitations in Extremum Seeking Control," Syst. Control Lett., **39**(5), pp. 313–326.
[24] Krstic, M., and Wang, H. H., 2000, "Stability of Extremum Seeking Feedback for General Nonlinear Dynamic Systems," Automatica, **36**(4), pp. 595–601.
[25] Liu, S. J., and Krstic, M., 2010, "Stochastic Averaging in Continuous Time and Its Applications to Extremum Seeking," IEEE Trans. Autom. Control, **55**(10), pp. 2235–2250.
[26] Liu, S. J., and Krstic, M., 2012, *Stochastic Averaging and Stochastic Extremum Seeking*, Springer Science & Business Media, Germany.
[27] Oliveira, T. R., Krstic, M., and Tsubakino, D., 2017, "Extremum Seeking for Static Maps With Delays," IEEE Trans. Autom. Control, **62**(4), pp. 1911–1926.
[28] Rušiti, D., Evangelisti, G., Oliveira, T. R., Gerdts, M., and Krstic, M., 2019, "Stochastic Extremum Seeking for Dynamic Maps With Delays," IEEE Control Syst. Lett., **3**(1), pp. 61–66.
[29] Tan, Y., Nešić, D., and Mareels, I., 2006, "On Non-Local Stability Properties of Extremum Seeking Control," Automatica, **42**(6), pp. 889–903.
[30] Tan, Y., Nešić, D., Mareels, I., and Astolfi, A., 2009, "On Global Extremum Seeking in the Presence of Local Extrema," Automatica, **45**(1), pp. 245–251.
[31] Wang, H. H., Yeung, S., and Krstic, M., 2000, "Experimental Application of Extremum Seeking on an Axial-Flow Compressor," IEEE Trans. Control Syst. Technol., **8**(2), pp. 300–309.
[32] Peterson, K. S., and Stefanopoulou, A. G., 2004, "Extremum Seeking Control for Soft Landing of an Electromechanical Valve Actuator," Automatica, **40**(6), pp. 1063–1069.

[33] Chang, Y. A., and Moura, S. J., 2009, "Air Flow Control in Fuel Cell Systems: An Extremum Seeking Approach," American Control Conference, St. Louis, MO, June 10–12, pp. 1052–1059.
[34] Bagheri, M., Krstic, M., and Naseradinmousavi, P., 2018, "Multivariable Extremum Seeking for Joint-Space Trajectory Optimization of a High-Degrees of Freedom Robot," ASME J. Dyn. Syst., Meas., Control, **140**(11), p. 111017.
[35] Dervisoglu, G., Gomes, G., Kwon, J., Horowitz, R., and Varaiya, P., 2009, "Automatic Calibration of the Fundamental Diagram and Empirical Observations on Capacity," Transportation Research Board 88th Annual Meeting, Vol. 15, Washington, DC, pp. 31–59.
[36] Fan, S., and Seibold, B., 2013, "Data-Fitted First-Order Traffic Models and Their Second-Order Generalizations: Comparison by Trajectory and Sensor Data," Transp. Res. Rec., **2391**(1), pp. 32–43.
[37] Carlson, R. C., Papamichail, I., Papageorgiou, M., and Messmer, A., 2010, "Optimal Motorway Traffic Flow Control Involving Variable Speed Limits and Ramp Metering," Transp. Sci., **44**(2), pp. 238–253.
[38] Hegyi, A., Schutter, B. D., and Hellendoorn, H., 2005, "Model Predictive Control for Optimal Coordination of Ramp Metering and Variable Speed Limits," Transp. Res. Part C, **13**(3), pp. 185–209.
[39] Karafyllis, I., and Papageorgiou, M., 2019, "Feedback Control of Scalar Conservation Laws With Application to Density Control in Freeways by Means of Variable Speed Limits," Automatica, **105**, pp. 228–236.
[40] Lu, X. Y., Varaiya, P., Horowitz, R., Su, D., and Shladover, S. E., 2011, "Novel Freeway Traffic Control With Variable Speed Limit and Coordinated Ramp Metering," Transp. Res. Rec., **2229**(1), pp. 55–65.
[41] Yu, H., and Krstic, M., 2019, "Traffic Congestion Control for Aw-Rascle-Zhang Model," Automatica, **100**, pp. 38–51.
[42] Yu, H., Diagne, M., Zhang, L., and Krstic, M., 2020, "Bilateral Boundary Control of Moving Shockwave in LWR Model of Congested Traffic," IEEE Trans. Autom. Control, epub.
[43] Zhang, Y., and Ioannou, P. A., 2017, "Coordinated Variable Speed Limit, Ramp Metering and Lane Change Control of Highway Traffic," IFAC-PapersOnLine, **50**(1), pp. 5307–5312.
[44] Hale, J. K., and Lunel, S. V., 1990, "Averaging in Infinite Dimensions," J. Integr. Equations Appl., **2**(4), pp. 463–494.
[45] Haring, M., and Johansen, T. A., 2017, "Asymptotic Stability of Perturbation-Based Extremum-Seeking Control for Nonlinear Plants," IEEE Trans. Autom. Control, **62**(5), pp. 2302–2317.
[46] Scheinker, A., and Krstic, M., 2014, "Extremum Seeking With Bounded Update Rates," Syst. Control Lett., **63**, pp. 25–31.
[47] Yu, H., Gan, Q., Bayen, A., and Krstic, M., 2020, "PDE Traffic Observer Validated on Freeway Data," IEEE Trans. Control Syst. Technol. epub.
[48] Krstic, M., and Smyshlyaev, A., 2008, *Boundary Control of PDEs: A Course on Backstepping Designs*, SIAM, Philadelphia, PA.